

Seasonal variation of floc population influenced by the presence of algae in the Changjiang (Yangtze River) Estuary

Deng, Zhirui; He, Qing; Chassagne, Claire; Wang, Zheng Bing

DOI

[10.1016/j.margeo.2021.106600](https://doi.org/10.1016/j.margeo.2021.106600)

Publication date

2021

Document Version

Accepted author manuscript

Published in

Marine Geology

Citation (APA)

Deng, Z., He, Q., Chassagne, C., & Wang, Z. B. (2021). Seasonal variation of floc population influenced by the presence of algae in the Changjiang (Yangtze River) Estuary. *Marine Geology*, 440, Article 106600. <https://doi.org/10.1016/j.margeo.2021.106600>

Important note

To cite this publication, please use the final published version (if applicable). Please check the document version above.

Copyright

Other than for strictly personal use, it is not permitted to download, forward or distribute the text or part of it, without the consent of the author(s) and/or copyright holder(s), unless the work is under an open content license such as Creative Commons.

Takedown policy

Please contact us and provide details if you believe this document breaches copyrights. We will remove access to the work immediately and investigate your claim.

1 Seasonal variation of floc population influenced by the presence
2 of algae in the Changjiang (Yangtze River) Estuary

3 Zhirui Deng^{a, b}, Qing He^{a, *}, Claire Chassagne^{b, c}, Zheng Bing Wang^{a, b, c}

4 ^a State Key Lab of Estuarine and Coastal Research, East China Normal University, Shanghai 200241,
5 China

6 ^b Section of Environmental Fluid Mechanics, Faculty of Civil Engineering and Geosciences, Delft
7 University of Technology, PO Box 5048, 2600, GA, Delft, The Netherlands

8 ^c Deltares, Delft, the Netherlands

9 * Corresponding author.

10 E-mail address: qinghe@sklec.ecnu.edu.cn (Q. He).

11 **Abstract**

12 The variation of the floc population in the Changjiang Estuary has been studied for both winter
13 and summer season as a function of the presence of living (micro)algae. The influence of algae has
14 been characterized through the use of the chlorophyll-a concentration to suspended sediment
15 concentration (CC/SSC) ratio. Two whole tidal cycle sampling campaigns were carried out and a
16 full set of parameters (particle size distribution, particle concentration, salinity, velocities,
17 chlorophyll-a concentration) was recorded as function of time for 6 vertical depths. It is found that
18 the floc population can be described by three particle classes. The two most dynamic classes
19 (microflocs and macroflocs) co-exist in the water column. It was nonetheless found, due to the
20 correlation between CC/SSC and particle sizes that the system is at steady state, both in summer
21 and in winter. This can be explained by the limited flocculation ability between the classes due to

22 their segregation in the water column. In winter, macroflocs are found at the top of the water column
23 but their amount and size are very reduced with a mean CC/SSC value of $13\pm 11 \mu\text{g g}^{-1}$. In summer,
24 algae-rich macroflocs are abundant at the top of the water column with a mean CC/SSC value of
25 $21\pm 18 \mu\text{g g}^{-1}$, especially at flood tide. Microflocs, on the other hand, have a higher density and are
26 generally found deeper in the water column. At high water slack, both macroflocs and microflocs
27 will settle but will never catch-up. The fact that the flocs are at steady-state in terms of flocculation
28 is of importance for sediment transport modelling.

29

30 Key words: Flocculation; Algae; Changjiang Estuary; Yangtze Estuary; Particle size distribution;
31 Floc size; Tidal variation; Seasonal variation

32 **1. Introduction**

33 Flocculation of fine sediment particles, resulting in time and space-dependent settling
34 velocities, plays an important role in the fine sediment dynamics in estuaries (van Leussen, 1988).
35 A large number of studies have been devoted to study flocculation, by field observations (Alldredge
36 and Gotschalk, 1989; Braithwaite et al., 2010; Fennessy and Dyer, 1996; Guo et al., 2017; Li et al.,
37 2017), laboratory measurements (Guan et al., 1996; Manning and Dyer, 1999; Wan et al., 2015) and
38 modelling (Khelifa and Hill, 2006; Mietta et al., 2011; Winterwerp, 1998).

39 Many factors can influence sediment flocculation and studies have concentrated on the
40 influence of shear rate (Keyvani and Strom, 2014; Manning and Dyer, 1999), SSC and salinity
41 (Eisma and Irion, 1993; Fettweis et al., 2010, 2007; Karbassi et al., 2014; Manning et al., 2010a,
42 2010b; Mietta et al., 2009a; Pérez et al., 2016; van Kessel et al., 2011). It has long been recognized

43 that in natural environments, organic matter is always part of flocs (Eisma et al., 1991). In that
44 review article, the authors confirm that the kinetics for flocculation are related to the tidal cycle, and
45 that microscope observations have shown that flocs consist of mineral particles held together by
46 organic matter (organic matter with or without hard parts of organisms). They state that in west-
47 European estuaries there is no evidence for an influence of salinity on in situ floc size distributions.
48 A same result was found for our site of interest, i.e. the Changjiang Estuary (Guo et al., 2017) and
49 the Seine estuary (Verney et al., 2009). As salt-induced flocculation is a slow process it will only be
50 dominant in the case that no other flocculating agent is present (like polyelectrolytes, stemming
51 from industry or produced by microorganisms) (Mietta et al., 2009a, 2009b). Salinity can however
52 influence the binding of organic matter to mineral clay (Wilkinson et al., 2017).

53 Polyelectrolytes like Extracellular Polymeric Substances (EPS) have been shown to drive
54 flocculation (Droppo, 2001; Furukawa et al., 2014; Lee et al., 2017; Paterson and Hagerthey, 2001;
55 Tolhurst et al., 2002; Uncles et al., 2010). EPS primarily consists of carbohydrates, proteins, nucleic
56 acids, and polymers, which can absorb fine sediment particles and change their surface property (Ni
57 et al., 2009; Sheng and Yu, 2006). When we refer to algae-induced flocculation in this article, it is
58 implied that EPS-induced flocculation (whereby the algae can produce EPS) is also accounted for.
59 There is a strong correlation between algae bloom season and flocculation, when higher temperature
60 and higher light intensity promote algae activity and EPS secretion enhance sediment particles
61 flocculation (Chen et al., 2005; Fettweis and Baeye, 2015; Lee et al., 2017; Shen et al., 2018; van
62 der Lee, 2000). Most research associated to algae effects usually focus on the algae bloom season
63 (spring season, from March to June). We wanted to investigate the role of algae in different seasons
64 (summer and winter). One of the purposes of the present article is to compare floc size distribution

65 in summer and winter, related to microalgae content of the flocs.

66 Most studies also rely on observations made using instrument at a fixed position above bed. In
67 our study, we performed measurements as function of both depth and time in order to highlight the
68 vertical variation in particle distributions and their composition in terms of algae content.

69 In our previous study, realized in summer (Deng et al., 2019), we already found that the living
70 microorganisms (algae) have a specific influence on flocculation in summer, outside the algae
71 bloom season, as function of different hydrodynamics conditions and position in the water column.
72 It was shown that the algae particles could participate in the flocculation process and a key
73 parameter—the sediment to chlorophyll concentrations ratio (CC/SSC) —was introduced that
74 reflected the dependence of flocculation on algae concentration. In particular, it was concluded from
75 the study that large algae flocs (> 100 microns) were formed in a region devoid of sediment particles
76 whereas the lowest size fraction (< 5 microns) is composed of sediment particles eroded from the
77 bed at high shear. The particle size distribution (PSD) but also composition in the water column is
78 therefore dynamic and changes with depth and hydrodynamic conditions. As sediment transport
79 models are relying on estimation of the particle density (to assess their settling velocity), it is
80 important to study the variations of floc properties in space and time.

81 In the present study, we compare the algae influence on flocculation in different seasonal
82 conditions (summer and winter), and show how the floc properties such as effect density and settling
83 velocity are changing with the seasons. Most of sediment accretion occurs in the flood season
84 (summer) while erosion occurs in the dry season (winter) in the Estuary Turbidity Maximum (ETM)
85 area of Changjiang Estuary (Li et al., 2018). It will therefore be interesting to compare the
86 dependence of CC/SSC ratio on shear, particle size and position in the water column in winter and

87 in summer. Typical questions we like to answer are:

88 – How is the floc size evolving as function of season and tidal cycle in the whole water column?

89 – How are floc properties (density, settling velocity, size) linked with sediment/algae ratio?

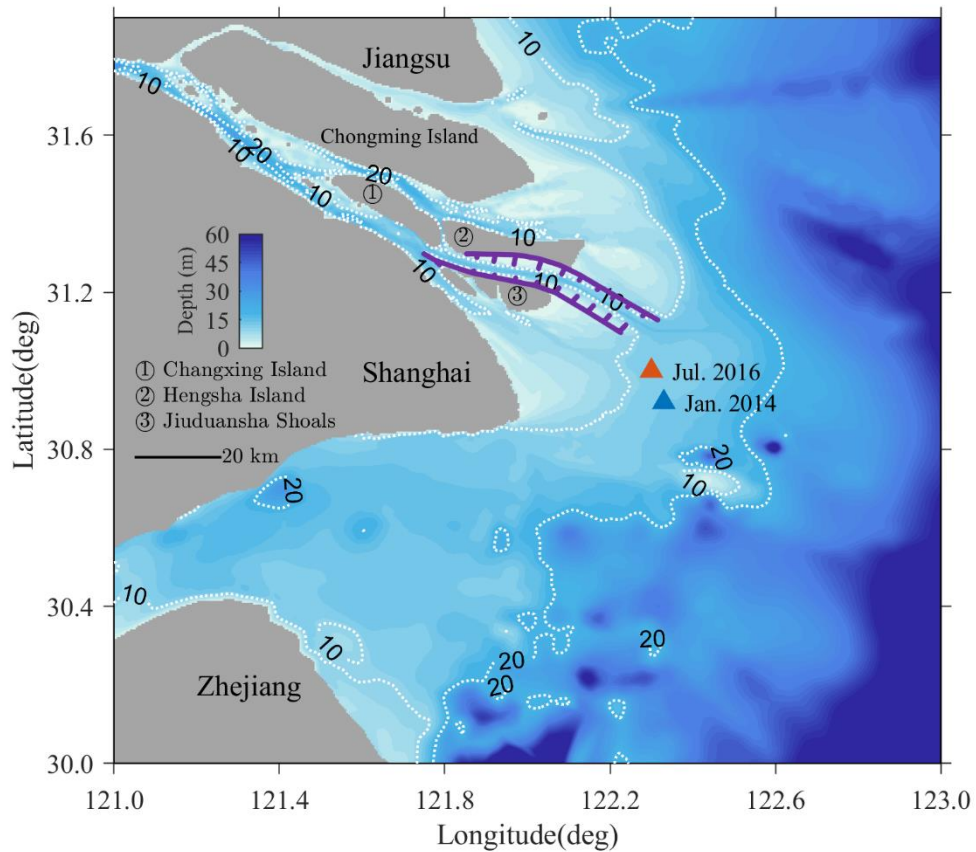
90 **2. Methodology**

91 **2.1 Site description**

92 Two full neap tidal cycle (13 h) sampling programs were carried out from 10th to 11th of January
93 2014 and 25th to 26th of July 2016 in the South Passage of Changjiang Estuary (Figure 1). River
94 discharges are about 11,000 m³ s⁻¹ during winter survey and 65,000 m³ s⁻¹ during summer survey,
95 respectively. There were no storms in the period before the observations, the tidal current that varied
96 with tidal phases was the main driver of turbulent shear.

97 In the Changjiang Estuary, the annual mean tidal range is about 2.6 m. The depth-averaged
98 velocity can reach up to 1 m s⁻¹ in surface water (Chen, 1995), and the depth-average velocity is
99 higher in summer (0.76–0.96 m s⁻¹) than winter (0.43–0.78 m s⁻¹) (Yun, 2004). The concentration
100 of chlorophyll-a (which is a proxy for algae concentration) in the South Passage and near the study
101 site has been given in Chen et al. (1999) and Wang et al. (2015) and the values are found to be in
102 the range 3–30 mg m⁻³ (= 3 to 30 µg l⁻¹) in surface water. The suspended sediments in the
103 Changjiang Estuary are mostly fine-grained particles (their amount can reach up to 95%). The
104 average D₅₀ of the suspended sediment is 7–11 µm, whereas the D₅₀ range of the top bed sediment
105 is 5.9–182.8 µm in the ETM zone. The average D₅₀ is 14.2 µm in South Passage area (although there
106 are spatial variations). In particular, most of sediment in the study site (located in South Passage)
107 has a D₅₀ of about 8.2 µm, and consists of clayed silt (about 20% clay, 70% silt and 10% sand) (Liu

108 et al., 2007). The Suspended Sediment Concentration (SSC) in the Changjiang Estuary varies
109 greatly over time and space, ranging from 0.1 to 20 g l⁻¹. The prevailing wind is in South-East
110 direction in summer with wind speeds of about 9.4 m s⁻¹. The prevailing wind in winter is in North-
111 West direction with wind speeds of about 7.4 m s⁻¹ (Yun, 2004).



112

113 *Figure 1 Map of the morphology of the Changjiang estuary and the study sites in summer (July in 2016) and*
114 *winter (January in 2014).*

115 2.2 Data acquisition

116 Each field survey was carried out with a multi-instruments device and covered a whole tidal
117 cycle. The device included the LISST-100C to measure particle size distribution and volume
118 concentration, OBS-3A for water turbidity, salinity, a multi-parameter water quality meter (Manta

119 2) for chlorophyll-a concentration and ADCP (300 kHz) for hydrodynamics. All the instruments
120 were attached together to make sure that all the detectors would measure at the same position. All
121 the instruments were set to record at an interval of 1 second. A full vertical profile was measured
122 every hour and the instruments were pulled slowly from bottom to surface at the speed of 0.05 m
123 s⁻¹. At specific locations in the water column, corresponding to the positions where the water
124 samples are taken (see underneath), the instruments were left for 2 min at the same position in order
125 to acquire statistically significant data. The data presented in the article is the average over the 2
126 min period. The hydrodynamic parameters were measured by ADCP (Acoustic Doppler Current
127 Profiler, 300 kHz), which was set up 0.5 m under the ship with a 1.71 m blanking distance and a
128 vertical resolution (bin size) of 0.5 m. Records of the water current direction and velocity were done
129 in real time, with an accuracy of $\pm 0.5\%/\pm 5\text{mm/s}$ (RD Instruments, 1994). Temperature and salinity
130 were also recorded.

131 In addition, water samples were collected by 1.2 L water sampler (horizontal trap sampler),
132 then divided into two glass bottles, one for SSC analysis (even hours) and another for chlorophyll-
133 a analysis or particle size analysis (the odd hours). We took these double water samples at 6 vertical
134 depths (0H, 0.2H, 0.4H, 0.6H, 0.8H, 1H) per hour. In our definition, 0 H represents the surface and
135 1 H the bottom. The height corresponding to 1 H was sampled 0.5 m above the bed. A water sample
136 for each height was filtered through a 0.45 μm cellulose acetate pre-weight filter paper, dried and
137 weighted to estimate the sediment concentration distribution through the water column.

138 **2.2.1 Particle Size Distribution and concentration**

139 The particle size distribution and volume concentration were recorded by LISST-100X with

140 the path length reduction module (PRM) of 90%. The LISST-100X is a submersible multi-parameter
141 system for in-situ measurements (Agrawal and Pottsmith, 2000; Pottsmith and Keir, 2013). A
142 particle size distribution and volume concentration were obtained by small-angle light scattering
143 (670 nm diode laser). The silicon detector has 32 specific log-spaced angle ranges. The raw data
144 was post-processed to obtain particle size distribution and volume concentration. The validity of the
145 data was assessed by checking the transmission value (of the raw data) which should be between
146 0.3 to 0.9 (Pottsmith, 2015). Furthermore we have thoroughly checked the data for a possible
147 schlieren effect (Mikkelsen et al., 2008), by comparing LISST and OBS data, and discarded the data
148 affected by it.

149 The OBS-3A (Optical Backscatter Sensor) is an optical sensor that measures turbidity and was
150 used, after calibration, to estimate the Suspended Sediment Concentration (SSC). The calibration
151 regression coefficients were: $R^2 = 0.9194$ in winter and $R^2 = 0.9439$ in summer, respectively.

152 **2.2.2 Chlorophyll-a concentration**

153 Chlorophyll-a is used as a proxy for determining the presence of algae (Knap et al., 1996). The
154 concentration of chlorophyll-a found in a water sample was used to estimate the concentration of
155 phytoplankton (algae) and was recorded with a Manta 2 instrument (Water Quality Multiprobe,
156 Eureka Environmental Engineering Company). Fluorescence sensors were used to induce
157 chlorophyll-a fluorescence by shining a beam of light of corresponding wavelength (435–470 nm)
158 into the water and then measuring the higher wavelength light which was emitted (Eureka
159 Environmental Engineering, 2016; Lamb et al., 2012). The laboratory chlorophyll-a analysis water
160 sample was filtered through a 0.45 μm ultra-fine glass fiber filter paper and stored at $-20\text{ }^\circ\text{C}$ for

161 chlorophyll-a measurements in laboratory. The calibration regression coefficients were: $R^2 =$
162 0.4960 in winter and $R^2 = 0.8337$ in summer, respectively. More details can be found in a
163 previous study (Deng et al., 2019).

164 **2.2.3 Complementary laboratory experiments**

165 The primary particles analysis was measured by Malvern Mastersizer 2000 laser granularity
166 analyzer (measurement ranges from 0.02–2000 μm , the repetition error is within 3%). Before the
167 instrument measurements, the water sample was handled with hydrogen peroxide (H_2O_2) and
168 hydrochloric acid (HCl) to remove the organic matter and carbonate. Hexametaphosphate
169 ($(\text{NaPO}_3)_6$) was then added as a dispersant and the sample was ultrasonically shaken (for 15
170 minutes).

171 **2.3 Data processing**

172 **2.3.1 Floc properties**

173 In this article, we will refer to “particles” or “flocs” but it should be understood that either
174 particles or flocs can be composed of (a) entirely mineral clay, (b) mineral clay – organic matter
175 aggregates (organic matter being algae and their produced EPS), (c) algae and algae aggregates.

176 The density $\Delta\rho$ of flocs was estimated from the LISST and OBS data, using equation (2)
177 (Fettweis, 2008; Verney et al., 2009):

$$\Delta\rho = \rho_F - \rho_W = \left(1 - \frac{\rho_W}{\rho_P}\right) \frac{SSC}{V_F} \quad (2)$$

178 Where ρ_F is the floc density, ρ_W is the water density which is calculated by one-atmosphere
179 equation of state of seawater (Millero and Poisson, 1981), ρ_P is the sediment particle density which

180 is estimated to 2650 g l⁻¹, *SSC* is the mass suspended sediment concentration obtained from the
181 OBS and V_F is the floc volume concentration from LISST.

182 The settling velocity was calculated according to Stokes' law:

$$\omega_s = \frac{D_{50}^2 \Delta \rho g}{18\mu} \quad (3)$$

183 Where μ is the viscosity of water, D_{50} is the mean particle diameter and g is the
184 gravity constant.

185 2.3.2 Shear rate

186 To estimate the shear stress in the water column, the velocity data should be converted into
187 shear rate G (Guo et al., 2017; Pejrup and Mikkelsen, 2010):

$$G(z, H, u_*) = \sqrt{\frac{u_*^3 \times (1 - z/H)}{\nu \kappa z}} \quad (4)$$

188 Where ν is the kinematic viscosity of the water [m² s⁻¹], H is the total water depth [m], z is
189 the height above bed, κ is Von Karman's constant (approximately 0.4) (Chien and Wan, 1999). The
190 friction velocity, u_* [m s⁻¹] is given by:

$$u_* = \frac{u(z) \times \kappa}{\ln\left(\frac{z}{z_0}\right)} \quad (5)$$

191 Where $u(z)$ is the current velocity amplitude [m s⁻¹] at position z . z_0 is assumed to be
192 constant and equal to 3 mm. This value has been used in other research of sediment transport in the
193 turbidity maxima of the Changjiang Estuary (e.g. Ge et al., 2012; Guo et al., 2017).

194 2.3.3 Algae-Sediment Ratio

195 Algae particles populate the whole water column and biomineral flocs have such a density that
196 these flocs settle to the bottom of the water column. This results in having a higher chlorophyll-a

197 concentration at the bottom than in the upper layer. Although some species of algae are adapted to
198 low light condition, most of algae would primarily be expected to be found in the upper water layer
199 as they rely on photosynthesis for their growth. This is especially the case for Skeletonema which
200 is the dominant algae species in Changjiang estuary, and which has an affinity with surface waters.
201 In order to scale the results with SSC, we defined a CC/SSC ratio to represent the algae relative
202 concentration (Deng et al., 2019):

$$Ratio = CC/SSC \quad (7)$$

203 where CC is the chlorophyll-a concentration [$\mu\text{g l}^{-1}$], SSC is the suspended sediment
204 concentration [g l^{-1}]. In Deng et al. (2019) it was in particular found that a high chlorophyll-a
205 concentration usually corresponds with high SSC in summer.

206 **3. Results and discussions**

207 Figure 2 and Figure 3 show the time series of the water hydrodynamics and flocculation
208 parameters during the winter and summer surveys, suspended sediment concentration (SSC),
209 salinity, chlorophyll-a concentration (CC) and floc size (D_{50}) were recorded. shear rate (G), floc
210 effective density ($\Delta\rho$), floc settling velocity (ω_s) were estimated using Eqs. (1,2,3).

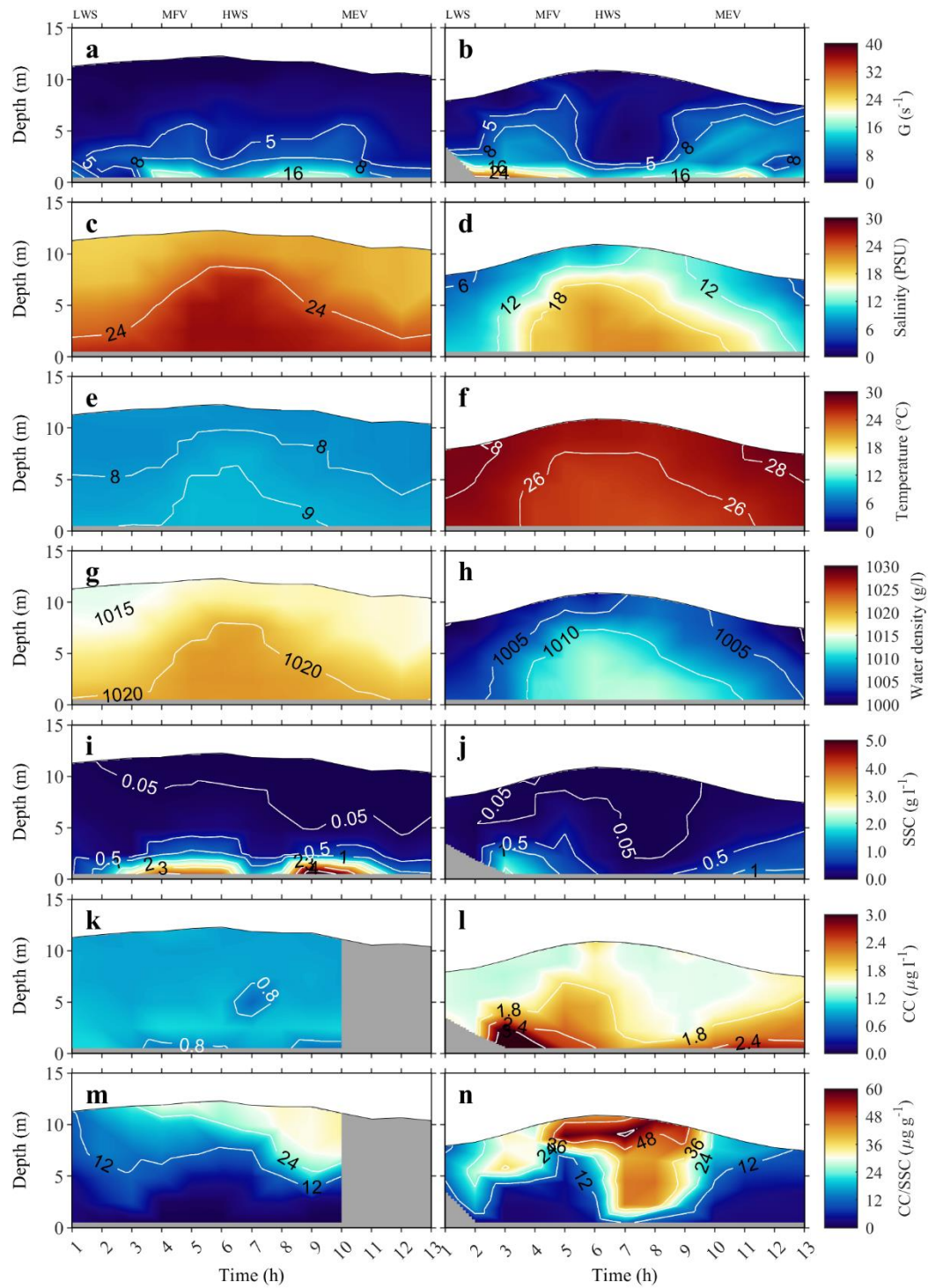
211 **3.1 Seasonal variations**

212 Each of the two surveys started from flood tide to ebb tide, lasted for 13 hours, and included a
213 whole tidal cycle with four periods: Low Water Slack (LWS), Maximum Flood Velocity (MFV),
214 High Water Slack (HWS) and Maximum Ebb Velocity (MEV).

215 The water depths as function as time demonstrated the tidal asymmetry with an ebb-dominance

216 that the flood periods are about 4 hours while the ebb periods are about 6 hours both in winter and
217 summer surveys. Because the observation station was further away from the coast in winter, the
218 water depth in winter (11–12.5 m) was deeper than in summer (7.5–11 m). The water depth variation
219 amplitudes in winter were smaller than in summer. The tidal range in winter was smaller than in
220 summer, which means that the hydrodynamics in winter are less energetic. This was also reflected
221 in the shear rate (Figure 2a, b). The shear rate ranged from 0.1–20 s⁻¹ in winter, and from 0.4–50 s
222 ⁻¹ in summer. The shear rate in summer was always higher than in winter for the same tidal period.
223 In addition, the shear rates remained at a high value at flood period and ebb period. The SSC
224 correlated with shear rate both in winter and summer surveys. The maximum SSC usually appeared
225 at the high shear rate periods (MFV and MEV). Although the SSC in bottom water was lower during
226 the summer survey than during the winter survey, the SSC in upper water was higher than during
227 the winter survey (> 0.05 g l⁻¹).

228 The salinity in winter was higher than in summer because of a smaller river discharge in winter
229 (Figure 2c, d). The salinity in winter ranged from 18.5 to 27.3 PSU (it increased with rising tide),
230 which means that the water column was mainly affected by sea water. The salinity ranged in summer
231 from 4.8 to 22.0 PSU meaning that the water column was always affected by both fresh and sea
232 water. The vertical gradient of salinity indicated different stratifications in winter and summer: water
233 is better mixed in winter than in summer. The stratification corresponded with high CC/SSC in
234 summer at the top of the water column, probably due to favorable algae growth conditions during
235 that period. These flocs are mainly advected from the sea at flood tide (Zhao and Gao, 2019).



236

237

Figure 2 Vertical distribution of shear stress (a, b), salinity (c, d), Temperature (e, f), water density (g, h),

238 *sediment concentration (i, j), chlorophyll-a concentration (k, l) and algae-sediment ratio (m, n).*

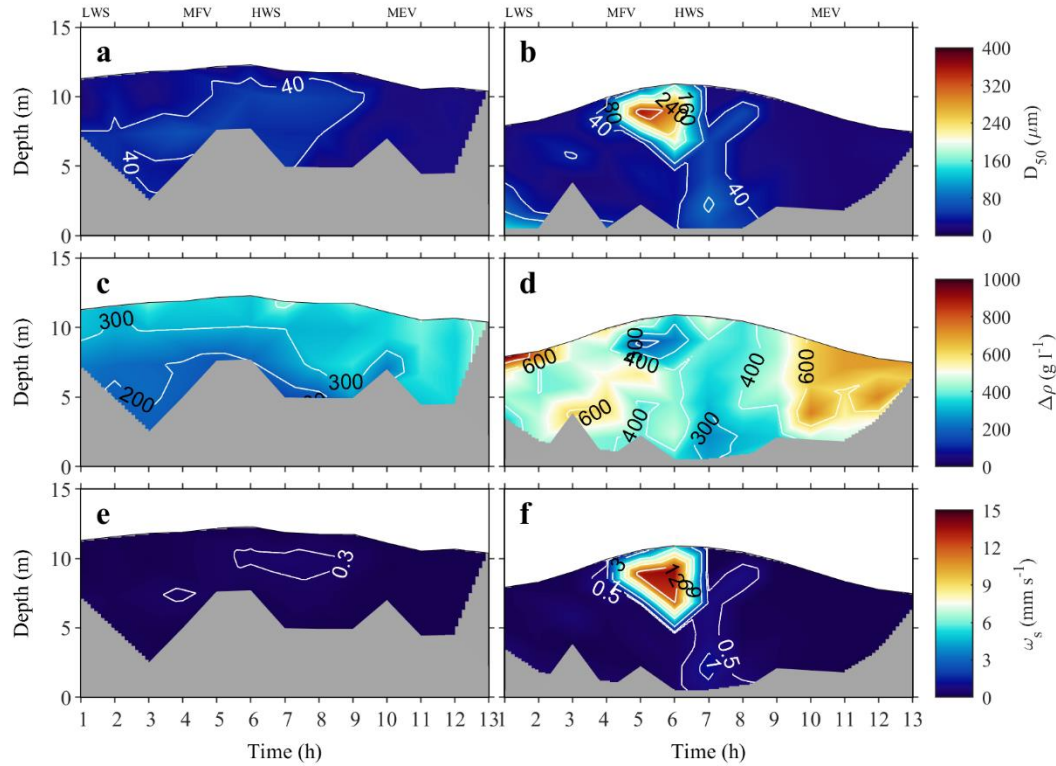
239 *(Left: 2014-01 winter season, Right:2016-07 summer.*

240 *LWS:1-2 h, MFV: 4-5 h, HWS: 6-7 h, MEV: 10-11 h).*

241 The temperature in winter (7–10 °C) was lower than in summer (25–29 °C) (Figure 2e, f). The
242 salinity is shown to correlate with the water density for both the winter and the summer survey
243 period: a high salinity corresponds to a high water density and vice-versa. There is no correlation
244 between SSC and water density as there is no correlation between SSC and salinity, a feature that
245 was already observed in diverse estuaries worldwide and this estuary in particular (Eisma et al.,
246 1991; Guo et al., 2017).

247 **3.2 Mean floc properties in winter and in summer**

248 In Figure 3 it is shown that the median floc size (D_{50}) in winter (13–65 μm) is smaller than in
249 summer (13–359 μm). Studies in the same area have shown that Particulate Organic Carbon (POC)
250 correlates positively with chlorophyll-a, and that the amount of POC is reduced in winter as
251 compared to summer (Zhao and Gao, 2019). This is in line with the results presented in Figure 2k,
252 l, where the CC is lower in winter as compared to summer. Flocculation induced by particulate
253 organic matter (as represented by POC) is therefore reduced in winter. Floccs of higher size can only
254 be observed if their effective density is low enough so that their residence time in the water column
255 is significant—this can only be achieved if floccs contain a substantial amount of algae.



256

257 **Figure 3 Vertical distribution of mean floc size (a, b), effective density (c, d) and settling (e, f) velocity. (Left:**

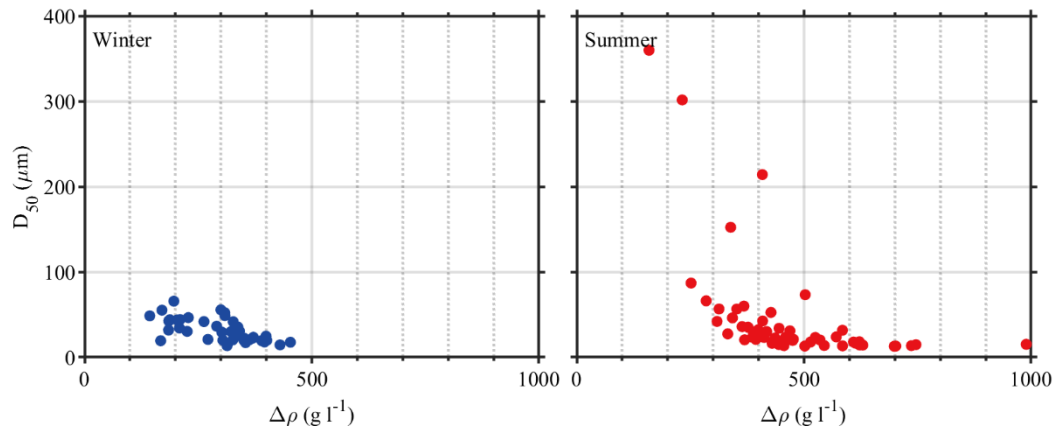
258 **2014-01 winter season, Right: 2016-07 summer, LWS: 1–2 h, MFV: 4–5 h, HWS: 6–7 h, MEV: 10–11 h)**

259 The effective floc density map shows that large particles are found in the upper layer, especially
 260 at HWS. These particles have a higher settling velocity than other particles found at the same time
 261 in the water column, but have a similar density. Particles of higher density are found (in all layers)
 262 when the shear rate is higher than in other periods (both around 8–12 h in winter and in summer).
 263 The mean floc size has a positive correlation with effective density in summer: large flocs usually
 264 have a smaller density, and vice versa. This is better represented in Figure 4. This result is consistent
 265 with many other studies where the relation between density and size is an exponentially decreasing
 266 function (Manning et al., 2006; Manning and Dyer, 1999; Mikkelsen et al., 2007). The mean
 267 effective density of flocs in winter appears to be a little smaller in winter than that in summer. This
 268 is counter-intuitive if one assumes that flocs in summer are composed of more algae than in winter

269 (which is confirmed by comparing the CC/SSC ratio in both seasons). However, as discussed in the
270 previous section, the shear rates were overall higher in summer than in winter. This has two effects:

271 1—the high shear rate in summer leads to more sediment resuspension during MFV, whereby
272 this sediment is flocculated by biological agents (EPS secreted by algae). Even silt-size particles
273 could be trapped in these flocculated structures, leading to flocs with higher density. These flocs
274 even reach the surface water (except for HWS periods), see section 3.3.2. As is shown in Figure 8,
275 the sediment that is in surface water in winter contains more clay-size particles than in summer,
276 which is due to both lower shear rates and lower organic material content in that season compared
277 to summer.

278 2—There can be a reformation of flocs under shear (a reduction in volume while sediment
279 mass is preserved) resulting in a higher density in summer (Guo, 2018; Sterling et al., 2004; Verney
280 et al., 2009; Winterwerp, 1998). This hypothesis is debatable as reformation is depending
281 strongly on residence time and the nature of the organic matter that composes the floc. The
282 composition of organic matter is known to be different in summer and winter (Hart et al., 1990;
283 Morrissey et al., 2014). The organic matter in summer is usually composed of living algae and their
284 EPS, which can capture effectively mineral sediment particles, leading to higher particle density
285 than in winter. In winter the organic matter is scarce and usually composed of debris and dead
286 organic matter or EPS (Craig et al., 1989; Grey et al., 2001).



287
288 **Figure 4 Correlation between effective density with mean flocc size**

289 The settling velocity is positively correlated with D_{50} and large flocs have a larger settling
290 velocity than small flocs; this is to be expected since the settling velocity is depending on the particle
291 size squared, whereas it is only linearly correlated with density, see Eq. (2) and that density is within
292 the limited range 140–990 g l^{-1} .

293 3.2.1 Variations with shear rate, salinity and SSC

294 There are many studies about the influence of shear rate (Keyvani and Strom, 2014; Mietta et
295 al., 2009a), of salinity (Pérez et al., 2016; Verney et al., 2009), and of SSC (Eisma and Li, 1993;
296 Milligan and Hill, 1998) on sediment flocculation. In the Changjiang Estuary, the correlations
297 between D_{50} and salinity/SSC are poor. In addition, the shear rate displays an overall negative
298 relationship with D_{50} , that is, large flocs usually appear at low shear rate periods (HWS), but the
299 coefficient of determination is poor ($R^2 < 0.5$) both in winter and summer. These poor correlations
300 are in line with previous studies (Deng et al., 2019; Guo et al., 2017).

301 Table 1 shows the variations of floc properties and velocity, salinity and SSC in winter and
302 summer, and comparisons to other results of North Passage (NP) in Changjiang Estuary in summer
303 season (Guo et al., 2017). The main difference was that there were larger flocs ($> 100 \mu\text{m}$) in summer

304 in the South Passage compared to the North Passage, especially in surface water, this can be seen
 305 by comparing Figure 3 with fig.2 in Guo et al.(2017). As the study area chosen in the South Passage
 306 was closer to the sea, the salinity was overall higher and the shear rate lower than in Guo et al.(2017).

307 *Table 1 Characteristics of flocs and velocity, salinity, SSC, CC and CC/SSC in the South Passage (winter and*
 308 *summer) and North Passage (summer)*

Parameters	Winter	Summer	North Passage*
D ₅₀ (µm)	32±13	45±64	43±10
Density (g l ⁻¹)	143–453	159–989	60–450
Settling (mm s ⁻¹)	0.02–0.4	0.05–14	0.08–0.3
Current Velocity (m s ⁻¹)	0.5±0.2	0.9±0.4	1.4
Salinity (PSU)	18.5–27.3	4.8–22.0	2–11
SSC (g l ⁻¹)	0.6±1.2	0.3±0.4	0.24±0.12
CC (µg l ⁻¹)	0.9±0.1	1.8±0.5	-
CC/SSC (µg g ⁻¹)	13±11	21±18	-

309 * Data from Guo et al. (2017).

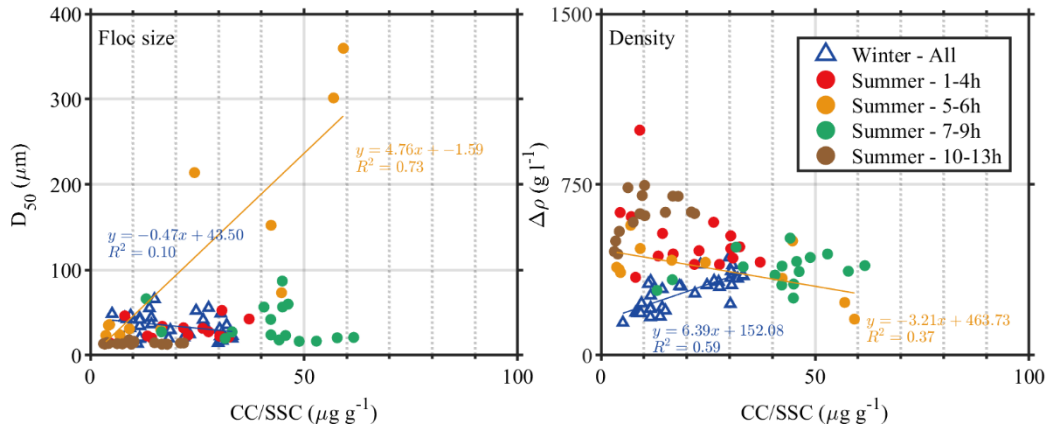
310 **3.2.2 Variation with CC and CC/SSC in the tidal cycle**

311 The chlorophyll-a concentration (CC) was relatively uniform over the whole water depth with
 312 a mean value of 0.9±0.1 µg l⁻¹ (0.6–1.0 µg l⁻¹) in winter and it was more stratified with higher
 313 concentrations towards the bed with a mean value of 1.5±0.5 µg l⁻¹ in summer (1.3–3.7 µg l⁻¹). It
 314 was observed that the CC in the bottom water is always higher than at the surface (also in winter).
 315 We will show (see Figure 11 and section 3.4.2) that a large amount of algae are binding to mineral
 316 clay by differential settling during the HWS period. This leads to an accumulation of algae and algae
 317 debris at the bed.

318 The CC/SSC ratio is shown in Figure 2m, n. The ranges of CC/SSC were around 0.1–33.2 µg
 319 g⁻¹ in winter and 1.5–61.6 µg g⁻¹ in summer, the higher values in upper water layer can reflect the
 320 vertical variation of algae activities. The correlation of CC with SSC in summer was already

321 discussed in (Deng et al., 2019). Even though the dataset presented here is of another summer (2015
322 in Deng et al. (2019) and 2016 in the present article), we found that the same conclusions hold. The
323 CC/SSC ratio plot illustrates that the algae percentage is higher in surface water, reflect that the
324 algae (CC) is not always distribute with sediment (SSC), they tend to stay in surface water, due to
325 their buoyancy or phototaxis. From Figure 2m, n, one finds that a threshold value for CC/SSC is
326 around 10–20 $\mu\text{g g}^{-1}$. Above this value, it is expected that flocs will be predominantly governed by
327 the organic matter (algae), as bimodal PSD are found. These type of flocs are found at the top of the
328 water column where algae can benefit from photosynthesis (Reynolds, 2006). During the summer
329 survey the algae-dominated flocs start to populate the whole water column in the period HWS to
330 ebb tide. At low hydrodynamic activity the buoyant algae particles in the water column are less
331 likely to flocculate with mineral sediment particles which will be predominantly found at the bottom
332 of the water column.

333 The trends for D_{50} as function of CC/SSC are shown in Figure 5. As was already observed in a
334 previous study (Deng et al., 2019), there is no correlation between D_{50} and CC/SSC in the summer
335 period (in 2015). It is confirmed that no overall trend is observed between D_{50} and CC/SSC in
336 summer (in 2016), nor in winter. There is however a marked increase in D_{50} with CC/SSC ratio
337 corresponding with low density particles at 5–6h in summer 2016, which indicates that the algae
338 play a significant role in large flocs formation during flood tide, when a lot of algae particles are
339 imported from the seaside. The details of algae effects on floc PSDs will be discussed in section 3.3
340 and 3.4.



341

342

Figure 5 D₅₀ and effective density as function of CC/SSC for winter and summer conditions

343

The density is better correlated with CC/SSC as can be seen in the Figure 5. The decreasing

344

trend observed in summer can be understood as a higher CC/SSC is then linked to a higher CC and

345

therefore a lower density (as in summer, SSC is relatively constant over the whole water column,

346

see Figure 2j). A higher CC/SSC ratio in winter corresponds to a lower SSC (as in winter, CC is

347

relatively constant over the whole water column, see Figure 2k), but as in winter there is a very low

348

CC and SSC, the correlation between density and CC/SSC is not to be trusted. The density is

349

nonetheless much lower than in summer for the same CC/SSC. We will come back to this point in

350

section 3.3.2.

351

3.3 Particle Size Distributions (PSD) during winter and summer surveys

352

Large flocs usually form at the upper part of the water column between MFV and HWS both

353

in winter and summer (Figure 3a, b). The vertical variation of flocs PSDs is however different in

354

winter and summer when one takes a closer look at the PSDs at different layers, see Figure 6. Flocs

355

are usually smaller in surface water (0 H) than in middle water (0.4 H) in winter at LWS (2 h) and

356

MFV (4 h) whereas they are small in summer for these periods. This implies that the flocculation

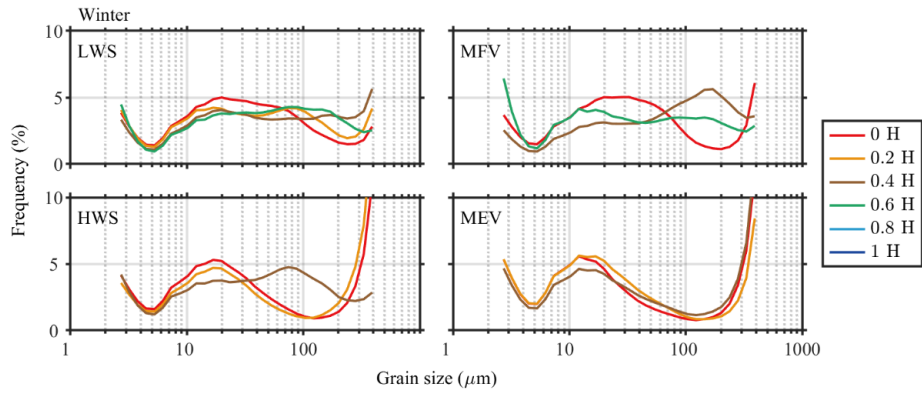
357

processes are different in winter and summer. Large flocs are hardly formed in summer in LWS (2

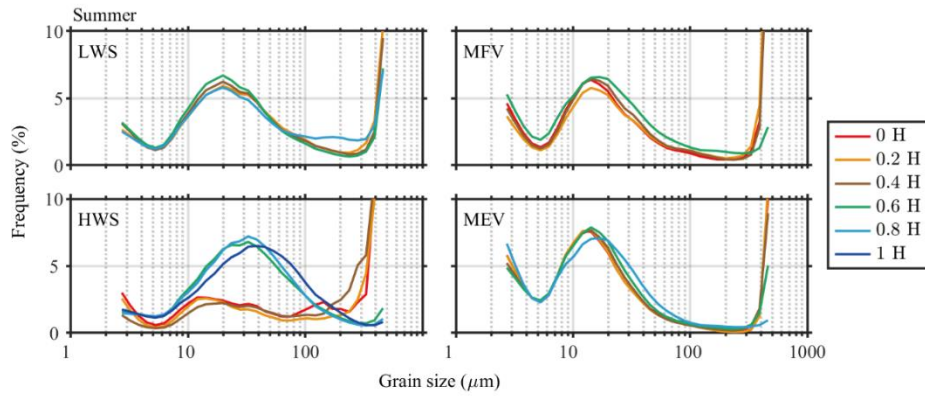
358 h), due to higher shear rates. Large flocs are formed at low shear rate both in winter and summer at
359 HWS (6 h). In particular, large flocs can be form in the middle and surface water in summer HWS.
360 This phenomenon will be discussed in the following section.

361 **3.3.1 Variation within the tidal cycle**

362 The PSD in winter at MFV is different from the other periods: at MFV the larger peak of the
363 PSD is found at 150 μm , whereas at the other periods it is around 20 μm . This behavior can be
364 ascribed to small sand particles that are eroded during maximum currents. In comparison, during
365 summer, the bed is more stabilized because of the presence of EPS and thus no large peak in MFV
366 is observed. The largest peak in summer is always around 20 μm at LWS, MFV and MEV, however
367 a second peak, around 100 μm , is distinguishable in three figures indicating the presence of particles
368 in that size range. This confirms the fact that in summer more organic particles, at all depths, are
369 present. At HWS (6 h), two PSDs are observed. Between [0 H–0.6 H], the PSD peaks at about 20
370 μm (with the peak having an asymmetric shape towards the highest sizes– again indicating the
371 presence of larger particles). Between [0.6 H–1 H] the PSD peaks at 30–50 μm and does not display
372 any large PSD asymmetry, but a significant amount particles in the range 100–400 μm .. This
373 transition seems to be in line with the change in salinity at HWS: clay-algae particles are probably
374 trapped under the pycnocline (see Figure 3j) whereas algae-rich particles are located above
375 (resulting in a large CC/SSC ratio, see Figure 3i). This trapping mechanism has also been reported
376 by other authors (Lee et al., 2016; Ren and Wu, 2014; Yao et al., 2016). The evolution of the PSD
377 around the changes in salinity gradients is shown in more details in Figure 7, reflecting the very
378 dynamic PSD's around HWS.



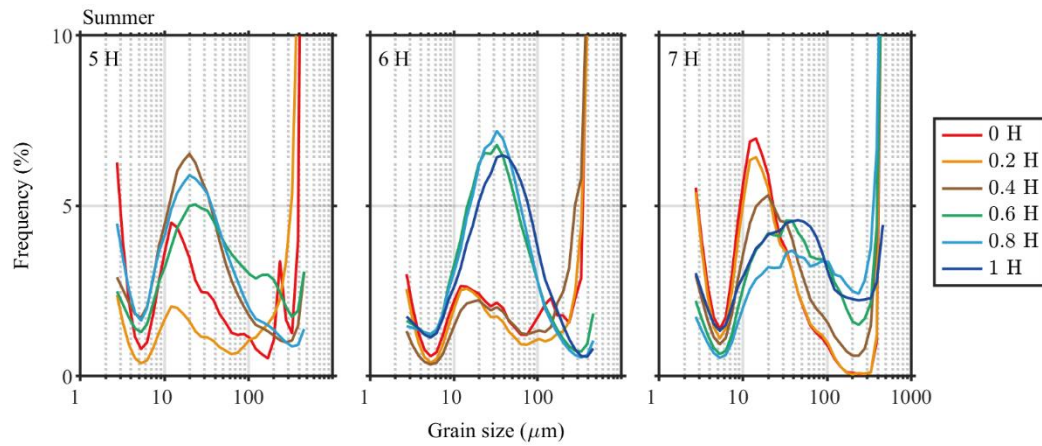
379



380

381 *Figure 6 Vertical variations of floc size distribution measured by LISST in different tidal phases, at neap tide.*

382 *The measurements are presented for LWS (2 h), MFV (4 h), HWS (6 h) and MEV (10 h).*



383

384 *Figure 7 Vertical variations of flocs PSDs in summer during the period 5–7 hours.*

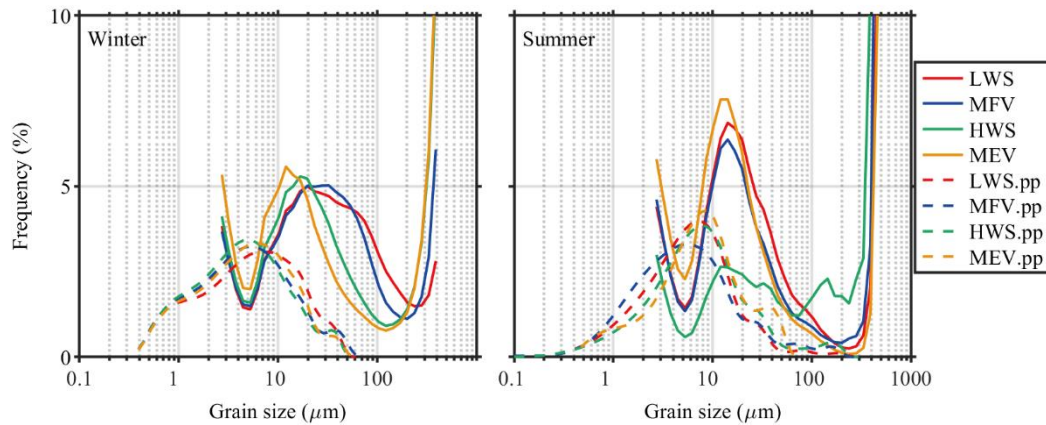
385 3.3.2 Particle characteristics at the top of the water column

386 The PSD of the particles collected at the top of the water column (in the surface water) was

387 further investigated by comparing the PSD measured in-situ and the PSD obtained in the laboratory

388 on samples treated so as to remove organic matter. These laboratory samples are labelled “primary
389 particles” (pp in short). The results are presented in Figure 8. It is found that primary particles in
390 summer ($D_{50} = 6 \mu\text{m}$) have the same mean size than in winter ($D_{50} = 5 \mu\text{m}$).

391 The PSD of the treated samples from the winter survey displays the presence of more fine clay-
392 size particles ($< 1 \mu\text{m}$) than in the samples from the summer survey. The difference can be explained
393 by the fact that in summer fine particles are more likely to be captured by organic matter and hence
394 be found at deeper depths. In winter fine particles (devoid of organic material) can populate the
395 whole water column. This very fine material cannot properly be recorded by LISST, as the lower
396 size range of the LISST is $2 \mu\text{m}$. A remarkable amount of large particles are found in the surface
397 water in-situ, both in summer and winter. These particles are usually not expected to be found in
398 surface waters if they are pure mineral particles (with a density close to 2600 g l^{-1}). We nonetheless
399 found, after treating the summer samples so as to remove organic matter, that large particles can still
400 be found (see Figure 8, summer, dashed lines). The nature of these particles is not known, they
401 might be skeletons of diatoms. Particles were monitored by LISST and OBS, from which particle
402 densities were deduced using equation (2). As LISST cannot properly measured the fine material in
403 the size range ($< 2 \mu\text{m}$) and that a significant amount of fine particles in that size range is found in
404 suspension in winter, the estimation of the density is biased. (see Supplementary information, where
405 the scattering in calibration lines for SSC in winter is shown). This results in the fact that flocs in
406 summer appear to have a higher density than flocs formed in winter as discussed at the end of section
407 3.2.2.



408

409 *Figure 8 Surface water size distribution of both dispersed (“pp”, i.e. measured in the lab after deflocculation)*

410

and flocculated particles (as measured in-situ) in different tidal phases.

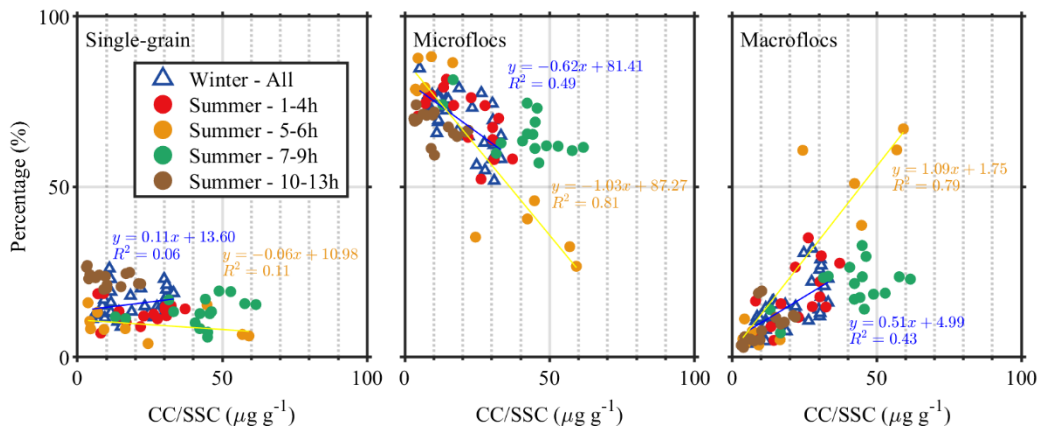
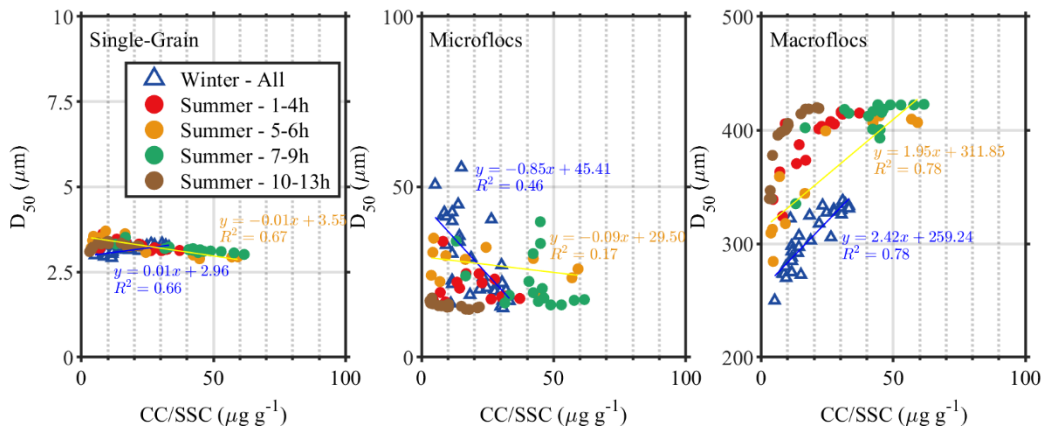
411 3.4 Floc classes

412 Following what other authors do, we subdivided the PSD into 3 classes: single-grain : particles
 413 of size < 5 μm, microflocs: particles of size > 5 μm and size < 200 μm and macroflocs of size > 200
 414 μm (Mikkelsen et al., 2006). It is expected, in light of the discussion in the previous sections, that
 415 single-grain particles are predominantly mineral based, macroflocs are composed in majority of
 416 organic material and microflocs are a combination of mineral sediment and algae.

417 3.4.1 Variation with CC/SSC

418 No correlation was found between CC/SSC and the D_{50} estimated from the whole PSD's. We
 419 here study the dependence of the D_{50} of each size class. The D_{50} of each class D_{50} as function of
 420 CC/SSC is given in Figure 9. From the figure, it can be seen that there is a correlation between D_{50}
 421 and CC/SSC: D_{50} of microflocs is decreasing with CC/SSC whereas the D_{50} of macroflocs is
 422 increasing. The volume-% of microflocs/macroflocs also display a clear trend with CC/SSC: the
 423 higher the CC/SSC, the more macroflocs are present in the water column. It was furthermore

424 verified (not shown) that the relative volume-% of macroflocs is decreasing with SSC. This is in
 425 line with the laboratory tests performed in Deng et al. (2019), where it was shown that the CC/SSC
 426 ratio is driving the steady-state size of the flocs: at higher CC/SSC ratio, larger flocs are obtained,
 427 irrespective of the amount of sediment or flocculant in presence. Algae sediment flocculation
 428 reaches a steady-state within 30 min in jar test experiments (Deng et al., 2019), for a large range of
 429 SSC (0.07–0.7 g l⁻¹) and a high shear rate (90 s⁻¹). This would hint to the fact that micro and
 430 macroflocs are (on average) at proper conditions that large flocs can be formed in HWS of summer,
 431 due to the HWS periods last about 2 hours with low shear rate.



434 *Figure 9 Relationship between the mean size D_{50} and volume % of each class with CC/SSC*

435 **3.4.2 Transfer between classes**

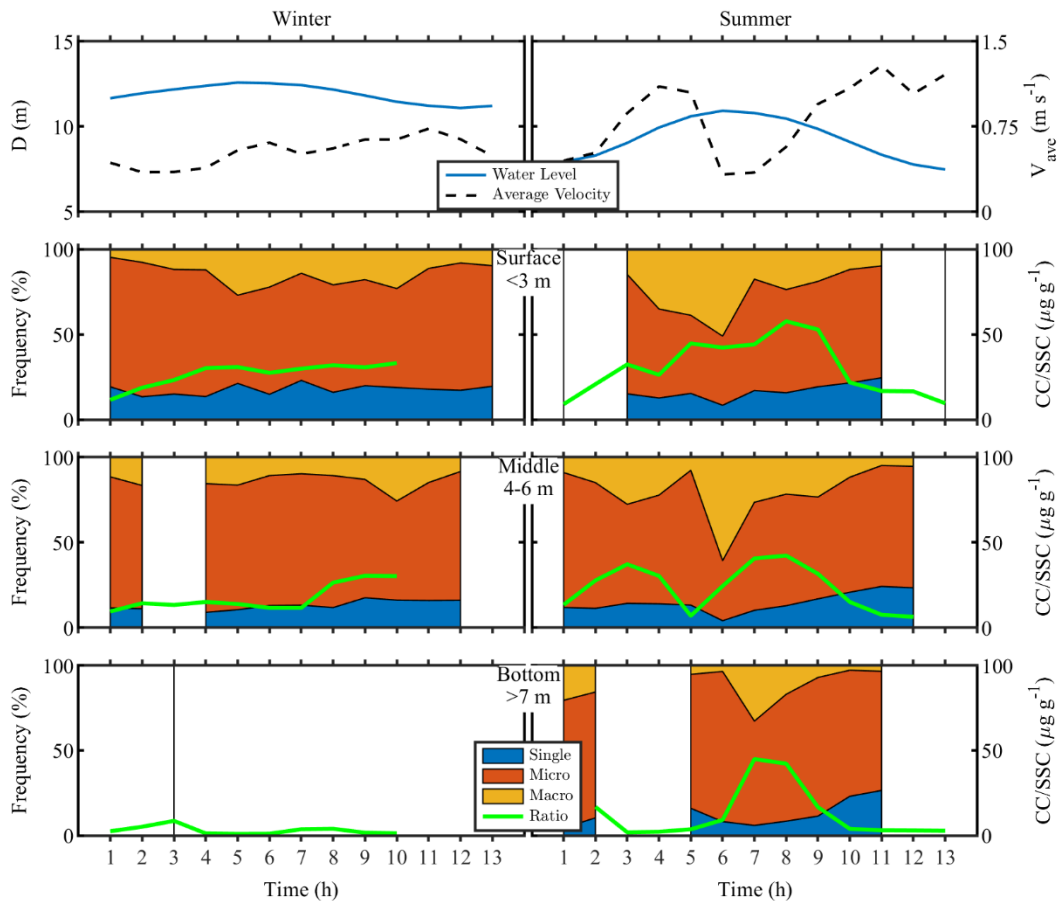
436 In sediment transport modelling, like in numerical programs such as TELEMAC (Blumberg et
437 al., 1996; Blumberg and Mellor, 1987), DELFT3D (Lesser et al., 2000, 2004) or ECOMSED
438 (Sherwood et al., 2018), two or three classes of particles are usually defined that are associated with
439 a concentration and a settling velocity. In the present article, we like to discuss the spatial and
440 temporal variation of the concentrations of the classes in terms of the relative volume fraction of
441 these classes that can be obtained from LISST data.

442 In section 3.4.1, it was shown that the CC/SSC ratio is correlated to the size of the micro and
443 macroflocs, which, as we discussed is an indication that the system is at steady-state.

444 Despite the fact that the system is at steady-state (in terms of flocculation), the PSD is very
445 dynamic and shifts between unimodal and bimodal depending on hydrodynamic conditions. This
446 shift is related to the relative volume-% of micro and macroflocs. A bimodal peak appears when the
447 two classes (microflocs and macroflocs) have a comparable relative volume fraction (volume-%).
448 The evolution of the % volume of the three classes and CC/SSC are given in Figure 10 as function
449 of time. The water column is divided in three: surface (0 H–0.2 H), middle (0.4 H–0.6 H) and bottom
450 (0.8 H–1 H). One can see that there is a slight increasing trend in CC/SSC from 11.6 to 33.2 $\mu\text{g g}^{-1}$
451 in surface water while no significant trend is found in other water layers during the tidal period in
452 winter. The CC/SSC ratio increases at flood tide in summer, at all depths (from 9 to 57.8 $\mu\text{g g}^{-1}$),
453 where a relative increase of the volume-% of macroflocs compared to the volume-% microflocs can
454 also be observed, which indicates that algae-rich particles are brought in the water column from the

455 sea. This is coherent with the observation made by Wu (2015) who observed that the dominant
456 species to be found at the observation station is Skeletonema which is found predominantly in sea
457 water.

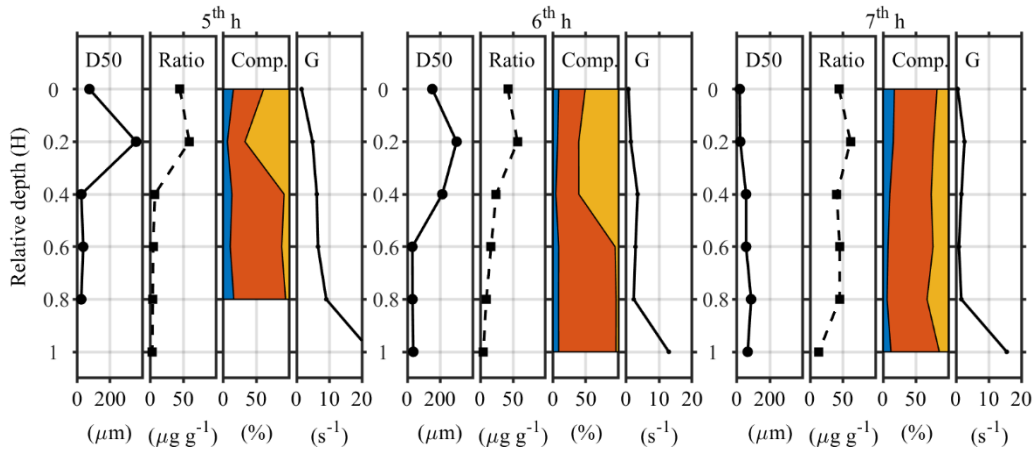
458 It is well-known that algae can aggregate in large flocs at the top of the water column where
459 they use sunlight to perform photosynthesis (Maggi and Tang, 2015; Takabayashi et al., 2006).
460 Subsequently, the algae-dominated flocs populate the whole water column in the period HWS to
461 ebb tide (see Figure 7 and Figure 11), slowly sinking to the bottom of the water column. As the
462 biomineral flocs are forming and settling, the CC/SSC ratio, which is about $50 \mu\text{g g}^{-1}$ at depths > 7
463 m increases below 7 m from 0 to $50 \mu\text{g g}^{-1}$ over time. This is to be linked with the observations
464 shown in Figure 2, where it was found that CC iso-lines are decreasing towards the bed over time
465 in that time period. This implies that a significant amount of algae is reaching the seafloor, and that
466 macroflocs are algae-dominated. It is known that algae flocs have a dynamic settling velocity, as
467 algae can adapt their buoyancy by photosynthetically-produced oxygen, therefore the CC/SSC ratio
468 remained high both in surface (0 H) and middle water (0.4 H), despite the settling of algae-based
469 flocs (Fernández-Méndez et al., 2014).



470

471 *Figure 10 Time series of three floc fractions with CC/SSC ratio in winter and summer season in surface, middle*
 472 *and bottom water layers*

473 The overall D_{50} is also changing over depth in time. At 6 h, during HWS, the largest D_{50} is
 474 shifting towards the middle depth, but its value is lower than at 5 h. At 7 h, the D_{50} is small
 475 everywhere, despite the fact that macroflocs are observed in the bottom layer: as the SSC is high in
 476 the bottom layer microflocs are the most abundant type of floc present, hereby reducing the overall
 477 D_{50} . As was observed in Figure 6, Figure 7 and Figure 8, the PSDs remain however bimodal,
 478 confirming the presence of large particles at any depth.



479

480 **Figure 11** Vertical variations of D_{50} , CC/SSC ratio, floc size fractions and shear rate in summer during the

481

period 5–7 hours.

482 It has been shown in Deng et al. (2019) that if the water column is well-mixed bimodal PSD's
 483 shift towards unimodal PSD's, as microflocs flocculate with macroflocs. This raises the question of
 484 residence in the water column, and the collision probability between micro and macroflocs. The
 485 variations in PSDs with depth in the period 5–7 hours (see Figure 11) was discussed above, where
 486 the clear difference between the PSDs found in the water column at [0 H–0.4 H] and [0.6 H–1 H]
 487 was attributed to the presence of a pycnocline: the residence time of algae flocs at specific depths
 488 are not only dependent on hydrodynamics but also on density—this is especially the case for algae-
 489 rich flocs which have smaller density than sediment dominated flocs. During HWS the algae flocs
 490 settle down, as do the mineral sediment particles and both have then no chance to meet as the slow
 491 settling algae flocs leaving the pycnocline do not catch-up with the faster settling sediment flocs
 492 that are found at lower depth. This can in part explain why multimodal PSDs are quite often
 493 observed in the system. Therefore, despite finding bimodal distributions, the flocculation ability
 494 between classes is very reduced and it can be concluded that the system is in good approximation
 495 at steady-state.

496 **4. Conclusions**

497 In this article, the seasonal variation of particle size distributions (PSD) were studied in relation
498 with the presence of living organic matter (algae). The presence of algae lead to both unimodal and
499 bimodal PSDs. When the PSD is bimodal two floc fractions (microflocs and macroflocs) can clearly
500 be distinguished. These two classes of flocs have different properties that can be studied as function
501 of relevant parameters (shear, CC/SSC ratio, seasonality). The existence of these two classes of
502 particles makes it therefore problematic to reduce the study of the PSD to the study of its D_{50} and it
503 was shown that no correlation could be found between the relevant parameters (CC/SSC in
504 particular) and D_{50} .

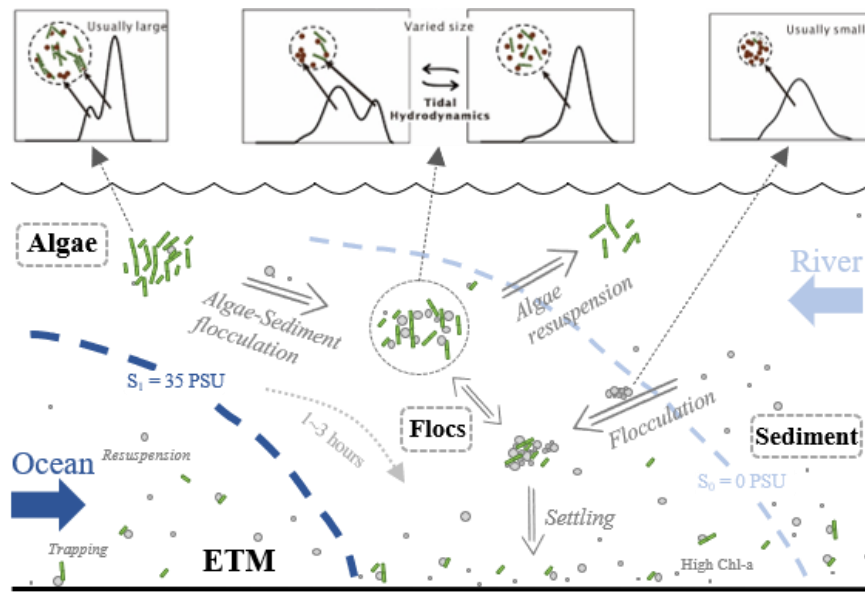
505 A clear difference is found between the winter and the summer surveys. Both the algae
506 production and the shear are low in winter, leading to the suspension of smaller flocs with lower
507 density than in summer (the average floc size is $32 \pm 13 \mu\text{m}$ in winter and $45 \pm 64 \mu\text{m}$ in summer, the
508 range density of flocs is $143\text{--}453 \text{ g l}^{-1}$ in winter and $159\text{--}989 \text{ g l}^{-1}$ in summer). The flocs are
509 composed of small amount of clay and organic particles in winter. In winter, more fine mineral
510 sediment (< 2 microns) are found at the top of the water column than in summer. In summer, the
511 flocs are larger by two orders of magnitude and can contain both clay and silt particles, which makes
512 them having a higher density than in winter, as in-situ monitoring techniques cannot properly assess
513 the very fine (< 2 microns) clay fraction suspended in winter. Moreover, as the shear rates were
514 higher in summer also, close to the bottom, larger silt and sand particles could be suspended
515 compared to winter.

516 A good correlation is found between the presence of algae (through the measurement of
517 chlorophyll-a concentration) and the presence of large, buoyant flocs at the top of the water column

518 in summer, where algae perform their photosynthesis. The algae appear predominantly during the
519 flood tide period. Large flocs, i.e. macroflocs, (with high CC/SSC ratio) are then formed during the
520 early flood period in the surface water. These flocs then settle to the middle water layer and finally
521 reach the bottom water layer during the HWS period. At the same time, microflocs with a higher
522 density than macroflocs are found deeper in the water column. During HWS both macroflocs and
523 microflocs settle down but cannot flocculate as they never catch-up due to the difference in settling
524 rates. This is the reason why, in line with the work of Soulsby et al. (2013), who studied Northern
525 European estuaries, it can be concluded that the floc population can be treated as if at steady state
526 in the Changjiang Estuary. This finding is of importance for the modelling of sediment transport in
527 this estuary, as the relative concentration of the microflocs/macroflocs populations at a given depth
528 is then solely governed by their settling rates and local hydrodynamic conditions (Manning et al.,
529 2010; Manning et al., 2011; Spearman et al., 2011; Spencer et al., 2010).

530 The algae-sediment interaction in the estuarine system is shown in Figure 12. The key factor
531 to study the changes in size, density and relative abundance of flocs are the CC/SSC ratio, which is
532 related to the volume-% fraction of micro and macroflocs. The full PSD's are changing with tidal
533 conditions and position in the water column (Figure 12), in line with our previous study (Deng et
534 al., 2019). In addition, due to the sensitivity of algae to their living environment, the floc
535 characteristics may vary from one location to another in the estuary. For example, in our previous
536 study, where the observation position was closer to the channel, the biological effect was weaker,
537 and combined with a strong estuarine tidal action, the distribution of floc sizes and settling velocities
538 were comparable during flood tide and ebb tide. In the present study the observation location was
539 closer to the open sea, the algae activity was relatively strong, and hence a strong tidal asymmetry

540 in floc size was observed, that is, flocs properties were clearly different at flood and ebb tide.



541

542

Figure 12 Algae-Sediment flocculation processes in estuary

543 Acknowledgements

544 This work is supported by the project 'Coping with deltas in transition' within the Programme of
545 Strategic Scientific Alliance between China and The Netherlands (PSA), financed by the Ministry
546 of Science and Technology, P.R. China (MOST) (No. 2016YFE0133700) and Royal Netherlands
547 Academy of Arts and Sciences (KNAW) (No. PSA-SA-E-02), and partly by the National Natural
548 Science Foundation of China (Nos. 51739005, 41876091) and Shanghai Committee of Science and
549 Technology (Nos. 19QA1402900; 20DZ1204700) and State Scholarship Fund of The China
550 Scholarship Council (No.201606140063). The study was carried out within the framework of the
551 MUDNET academic network: <https://www.tudelft.nl/mudnet/>.

552

553 Data Availability

554 Part of datasets related to this article can be found at <http://dx.doi.org/10.17632/pdfxj2mkp3>, an

555 open-source online data repository hosted at Mendeley Data (Deng, Zhirui, “Seasonal variation of
556 flocculation population influenced by the presence of algae in the Changjiang Estuary: Datasets and
557 Supplementary Materials”, 2021, Mendeley Data). Due to the confidentiality agreement of relevant
558 projects, more data that support the findings of this study are available from the corresponding
559 author, [Q.], upon reasonable request.

560 **Conflict of interest**

561 The authors declared that they have no conflicts of interest to this work.

562 **Reference**

- 563 Agrawal, Y.C., Pottsmith, H.C., 2000. Instruments for particle size and settling velocity observations
564 in sediment transport. *Marine Geology* 168, 89–114. [https://doi.org/10.1016/S0025-3227\(00\)00044-X](https://doi.org/10.1016/S0025-3227(00)00044-X)
565
- 566 Alldredge, A.L., Gotschalk, C.C., 1989. Direct observations of the mass flocculation of diatom
567 blooms: characteristics, settling velocities and formation of diatom aggregates. *Deep Sea
568 Research Part A. Oceanographic Research Papers* 36, 159–171.
569 [https://doi.org/10.1016/0198-0149\(89\)90131-3](https://doi.org/10.1016/0198-0149(89)90131-3)
- 570 Blumberg, A.F., Ji, Z.-G., Ziegler, C.K., 1996. Modeling outfall plume behavior using far field
571 circulation model. *Journal of Hydraulic Engineering* 122, 610–616.
572 [https://doi.org/10.1061/\(ASCE\)0733-9429\(1996\)122:11\(610\)](https://doi.org/10.1061/(ASCE)0733-9429(1996)122:11(610))
- 573 Blumberg, A.F., Mellor, G.L., 1987. A description of a three-dimensional coastal ocean circulation
574 model, in: Heaps, N.S. (Ed.), *Coastal and Estuarine Sciences*. American Geophysical Union,
575 Washington, D. C., pp. 1–16. <https://doi.org/10.1029/CO004p0001>
- 576 Braithwaite, K.M., Bowers, D.G., Nimmo Smith, W.A.M., Graham, G.W., Agrawal, Y.C.,
577 Mikkelsen, O.A., 2010. Observations of particle density and scattering in the Tamar Estuary.
578 *Marine Geology* 277, 1–10. <https://doi.org/10.1016/j.margeo.2010.06.008>
- 579 Chen, J., 1995. Sediment dynamics and evolution of the mouthbar and subaqueous delta in the
580 Yangtze estuary. *Resources & Environment in the Yangtze Valley*.
- 581 Chen, J., Li, D., Chen, B., Hu, F., Zhu, H., Liu, C., 1999. The processes of dynamic sedimentation
582 in the Changjiang Estuary. *Journal of Sea Research* 41, 129–140.
583 [https://doi.org/10.1016/S1385-1101\(98\)00047-1](https://doi.org/10.1016/S1385-1101(98)00047-1)
- 584 Chen, M.S., Wartel, S., Temmerman, S., 2005. Seasonal variation of flocculation characteristics on tidal
585 flats, the Scheldt estuary. *Hydrobiologia* 540, 181–195. <https://doi.org/10.1007/s10750-004-7143-6>
586
- 587 Chien, N., Wan, Z., 1999. *Mechanics of Sediment Transport*. American Society of Civil Engineers,
588 Reston, VA.

589 Craig, D., Ireland, R.J., Bärlocher, F., 1989. Seasonal variation in the organic composition of
590 seafoam. *Journal of Experimental Marine Biology and Ecology* 130, 71–80.
591 [https://doi.org/10.1016/0022-0981\(89\)90019-1](https://doi.org/10.1016/0022-0981(89)90019-1)

592 Deng, Z., He, Q., Safar, Z., Chassagne, C., 2019. The role of algae in fine sediment flocculation: In-
593 situ and laboratory measurements. *Marine Geology* 413, 71–84.
594 <https://doi.org/10.1016/j.margeo.2019.02.003>

595 Droppo, I.G., 2001. Rethinking what constitutes suspended sediment. *Hydrological Processes* 15,
596 1551–1564. <https://doi.org/10.1002/hyp.228>

597 Eisma, D., Bernard, P., Cadée, G.C., Ittekkot, V., Kalf, J., Laane, R., Martin, J.M., Mook, W.G., van
598 Put, A., Schuhmacher, T., 1991. Suspended-matter particle size in some West-European
599 estuaries; part II: a review on floc formation and break-up. *Netherlands Journal of Sea
600 Research* 28, 215–220. [https://doi.org/10.1016/0077-7579\(91\)90018-V](https://doi.org/10.1016/0077-7579(91)90018-V)

601 Eisma, D., Irion, G., 1993. Suspended Matter and Sediment Transport, in: Salomons, W., Bayne,
602 B.L., Duursma, E.K., Förstner, U. (Eds.), *Pollution of the North Sea*. Springer Berlin
603 Heidelberg, Berlin, Heidelberg, pp. 20–35. https://doi.org/10.1007/978-3-642-73709-1_2

604 Eisma, D., Li, A., 1993. Changes in suspended-matter floc size during the tidal cycle in the dollard
605 estuary. *Netherlands Journal of Sea Research* 31, 107–117. [https://doi.org/10.1016/0077-7579\(93\)90001-9](https://doi.org/10.1016/0077-7579(93)90001-9)

606

607 Eureka Environmental Engineering, I., 2016. *Manta 2 Water Quality Multiprobe Manual*.

608 Fennessy, M.J., Dyer, K.R., 1996. Floc population characteristics measured with INSSEV during
609 the Elbe estuary intercalibration experiment. *Journal of Sea Research* 36, 55–62.
610 [https://doi.org/10.1016/S1385-1101\(96\)90771-6](https://doi.org/10.1016/S1385-1101(96)90771-6)

611 Fernández-Méndez, M., Wenzhöfer, F., Peeken, I., Sørensen, H.L., Glud, R.N., Boetius, A., 2014.
612 Composition, Buoyancy Regulation and Fate of Ice Algal Aggregates in the Central Arctic
613 Ocean. *PLoS ONE* 9, e107452. <https://doi.org/10.1371/journal.pone.0107452>

614 Fettweis, M., 2008. Uncertainty of excess density and settling velocity of mud flocs derived from
615 in situ measurements. *Estuarine, Coastal and Shelf Science* 78, 426–436.
616 <https://doi.org/10.1016/j.ecss.2008.01.007>

617 Fettweis, M., Baeye, M., 2015. Seasonal variation in concentration, size, and settling velocity of
618 muddy marine flocs in the benthic boundary layer. *Journal of Geophysical Research:
619 Oceans* 120, 5648–5667. <https://doi.org/10.1002/2014JC010644>

620 Fettweis, M., Francken, F., Van den Eynde, D., Verwaest, T., Janssens, J., Van Lancker, V., 2010.
621 Storm influence on SPM concentrations in a coastal turbidity maximum area with high
622 anthropogenic impact (southern North Sea). *Continental Shelf Research* 30, 1417–1427.
623 <https://doi.org/10.1016/j.csr.2010.05.001>

624 Fettweis, M., Nechad, B., Van den Eynde, D., 2007. An estimate of the suspended particulate matter
625 (SPM) transport in the southern North Sea using SeaWiFS images, in situ measurements
626 and numerical model results. *Continental Shelf Research* 27, 1568–1583.
627 <https://doi.org/10.1016/j.csr.2007.01.017>

628 Furukawa, Y., Reed, A.H., Zhang, G., 2014. Effect of organic matter on estuarine flocculation: a
629 laboratory study using montmorillonite, humic acid, xanthan gum, guar gum and natural
630 estuarine flocs. *Geochemical Transactions* 15, 1. <https://doi.org/10.1186/1467-4866-15-1>

631 Ge, J., Chen, C., Qi, J., Ding, P., Beardsley, R.C., 2012. A dike–groyne algorithm in a terrain-
632 following coordinate ocean model (FVCOM): Development, validation and application.

633 Ocean Modelling 47, 26–40. <https://doi.org/10.1016/j.ocemod.2012.01.006>

634 Grey, J., Jones, R.I., Sleep, D., 2001. Seasonal changes in the importance of the source of organic
635 matter to the diet of zooplankton in Loch Ness, as indicated by stable isotope analysis.
636 *Limnology and Oceanography* 46, 505–513. <https://doi.org/10.4319/lo.2001.46.3.0505>

637 Guan, X., Chen, Y., Du, X., 1996. Experimental study on mechanism of flocculation in Yangtze
638 estuary (in Chinese). *Journal of Hydraulic Engineering* 1, 70–80.

639 Guo, C., 2018. Cohesive Sediment Flocculation and Settling Processes and the Controlling
640 Mechanisms (in Chinese) (PhD). East China Normal University, Shanghai.

641 Guo, C., He, Q., Guo, L., Winterwerp, J.C., 2017. A study of in-situ sediment flocculation in the
642 turbidity maxima of the Yangtze Estuary. *Estuarine, Coastal and Shelf Science* 191, 1–9.
643 <https://doi.org/10.1016/j.ecss.2017.04.001>

644 Hart, B.T., Bailey, P., Edwards, R., Hortle, K., James, K., McMahon, A., Meredith, C., Swadling,
645 K., 1990. Effects of salinity on river, stream and wetland ecosystems in Victoria, Australia.
646 *Water Research* 24, 1103–1117. [https://doi.org/10.1016/0043-1354\(90\)90173-4](https://doi.org/10.1016/0043-1354(90)90173-4)

647 Karbassi, A.R., Heidari, M., Vaezi, A.R., Samani, A.R.V., Fakhraee, M., Heidari, F., 2014. Effect of
648 pH and salinity on flocculation process of heavy metals during mixing of Aras River water
649 with Caspian Sea water. *Environmental Earth Sciences* 72, 457–465.
650 <https://doi.org/10.1007/s12665-013-2965-z>

651 Keyvani, A., Strom, K., 2014. Influence of cycles of high and low turbulent shear on the growth rate
652 and equilibrium size of mud flocs. *Marine Geology* 354, 1–14.
653 <https://doi.org/10.1016/j.margeo.2014.04.010>

654 Khelifa, A., Hill, P.S., 2006. Models for effective density and settling velocity of flocs. *Journal of*
655 *Hydraulic Research* 44, 390–401. <https://doi.org/10.1080/00221686.2006.9521690>

656 Knap, A., Michaels, A., Close, A., Ducklow, H., Dickson, A., 1996. Protocols for the Joint Global
657 Ocean Flux Study (JGOFS) Core Measurements.

658 Lamb, J.J., Eaton-Rye, J.J., Hohmann-Marriott, M.F., 2012. An LED-based fluorometer for
659 chlorophyll quantification in the laboratory and in the field. *Photosynthesis Research* 114,
660 59–68. <https://doi.org/10.1007/s11120-012-9777-y>

661 Lee, B.J., Hur, J., Toorman, E.A., 2017. Seasonal variation in flocculation potential of river water:
662 roles of the organic matter pool. *Water* 9, 335. <https://doi.org/10.3390/w9050335>

663 Lee, J., Liu, J.T., Hung, C.-C., Lin, S., Du, X., 2016. River plume induced variability of suspended
664 particle characteristics. *Marine Geology* 380, 219–230.
665 <https://doi.org/10.1016/j.margeo.2016.04.014>

666 Lesser, G., Van Kester, J., Roelvink, J., 2000. On-line sediment transport within Delft3D-FLOW.
667 Deltares (WL).

668 Lesser, G.R., Roelvink, J.A., van Kester, J.A.T.M., Stelling, G.S., 2004. Development and validation
669 of a three-dimensional morphological model. *Coastal Engineering* 51, 883–915.
670 <https://doi.org/10.1016/j.coastaleng.2004.07.014>

671 Li, D., Li, Y., Xu, Y., 2017. Observations of distribution and flocculation of suspended particulate
672 matter in the Minjiang River Estuary, China. *Marine Geology* 387, 31–44.
673 <https://doi.org/10.1016/j.margeo.2017.03.006>

674 Li, Y., Jia, J., Zhu, Q., Cheng, P., Gao, S., Wang, Y.P., 2018. Differentiating the effects of advection
675 and resuspension on suspended sediment concentrations in a turbid estuary. *Marine*
676 *Geology* 403, 179–190. <https://doi.org/10.1016/j.margeo.2018.06.001>

677 Maggi, F., Tang, F.H.M., 2015. Analysis of the effect of organic matter content on the architecture
678 and sinking of sediment aggregates. *Marine Geology* 363, 102–111.
679 <https://doi.org/10.1016/j.margeo.2015.01.017>

680 Manning, A.J., Bass, S.J., Dyer, K.R., 2006. Floc properties in the turbidity maximum of a mesotidal
681 estuary during neap and spring tidal conditions. *Marine Geology* 235, 193–211.
682 <https://doi.org/10.1016/j.margeo.2006.10.014>

683 Manning, A.J., Baugh, J.V., Spearman, J.R., Pidduck, E.L., Whitehouse, R.J.S., 2011. The settling
684 dynamics of flocculating mud-sand mixtures: Part 1—Empirical algorithm development.
685 *Ocean Dynamics* 61, 311–350. <https://doi.org/10.1007/s10236-011-0394-7>

686 Manning, A.J., Baugh, J.V., Spearman, J.R., Whitehouse, R.J.S., 2010a. Flocculation settling
687 characteristics of mud: sand mixtures. *Ocean Dynamics* 60, 237–253.
688 <https://doi.org/10.1007/s10236-009-0251-0>

689 Manning, A.J., Dyer, K.R., 1999. A laboratory examination of floc characteristics with regard to
690 turbulent shearing. *Marine Geology* 160, 147–170. [https://doi.org/10.1016/s0025-3227\(99\)00013-4](https://doi.org/10.1016/s0025-3227(99)00013-4)

692 Manning, A.J., Langston, W.J., Jonas, P.J.C., 2010b. A review of sediment dynamics in the Severn
693 Estuary: Influence of flocculation. *Marine Pollution Bulletin* 61, 37–51.
694 <https://doi.org/10.1016/j.marpolbul.2009.12.012>

695 Mietta, F., Chassagne, C., Manning, A.J., Winterwerp, J.C., 2009a. Influence of shear rate, organic
696 matter content, pH and salinity on mud flocculation. *Ocean Dynam* 59, 751–763.
697 <https://doi.org/10.1007/s10236-009-0231-4>

698 Mietta, F., Chassagne, C., Verney, R., Winterwerp, J.C., 2011. On the behavior of mud floc size
699 distribution: model calibration and model behavior. *Ocean Dynamics* 61, 257–271.
700 <https://doi.org/10.1007/s10236-010-0330-2>

701 Mietta, F., Chassagne, C., Winterwerp, J.C., 2009b. Shear-induced flocculation of a suspension of
702 kaolinite as function of pH and salt concentration. *Journal of Colloid and Interface Science*
703 336, 134–141. <https://doi.org/10.1016/j.jcis.2009.03.044>

704 Mikkelsen, O.A., Hill, P.S., Milligan, T.G., 2007. Seasonal and spatial variation of floc size, settling
705 velocity, and density on the inner Adriatic Shelf (Italy). *Continental Shelf Research* 27,
706 417–430. <https://doi.org/10.1016/j.csr.2006.11.004>

707 Mikkelsen, O.A., Hill, P.S., Milligan, T.G., 2006. Single-grain, microfloc and macrofloc volume
708 variations observed with a LISST-100 and a digital floc camera. *Journal of Sea Research*
709 55, 87–102. <https://doi.org/10.1016/j.seares.2005.09.003>

710 Mikkelsen, O.A., Milligan, T.G., Hill, P.S., Chant, R.J., Jago, C.F., Jones, S.E., Krivtsov, V.,
711 Mitchelson-Jacob, G., 2008. The influence of Schlieren on in situ optical measurements
712 used for particle characterization. *Limnology and Oceanography: Methods* 6, 133–143.
713 <https://doi.org/10.4319/lom.2008.6.133>

714 Millero, F.J., Poisson, A., 1981. International one-atmosphere equation of state of seawater. *Deep*
715 *Sea Research Part A. Oceanographic Research Papers* 28, 625–629.
716 [https://doi.org/10.1016/0198-0149\(81\)90122-9](https://doi.org/10.1016/0198-0149(81)90122-9)

717 Milligan, T.G., Hill, P.S., 1998. A laboratory assessment of the relative importance of turbulence,
718 particle composition, and concentration in limiting maximal floc size and settling behaviour.
719 *Journal of Sea Research* 39, 227–241. [https://doi.org/10.1016/S1385-1101\(97\)00062-2](https://doi.org/10.1016/S1385-1101(97)00062-2)

720 Morrissey, E.M., Gillespie, J.L., Morina, J.C., Franklin, R.B., 2014. Salinity affects microbial

721 activity and soil organic matter content in tidal wetlands. *Global Change Biology* 20, 1351–
722 1362. <https://doi.org/10.1111/gcb.12431>

723 Ni, B., Fang, F., Xie, W., Sun, M., Sheng, G., Li, W., Yu, H., 2009. Characterization of extracellular
724 polymeric substances produced by mixed microorganisms in activated sludge with gel-
725 permeating chromatography, excitation–emission matrix fluorescence spectroscopy
726 measurement and kinetic modeling. *Water Research* 43, 1350–1358.
727 <https://doi.org/10.1016/j.watres.2008.12.004>

728 Paterson, D.M., Hagerthey, S.E., 2001. Microphytobenthos in Constrasting Coastal Ecosystems:
729 Biology and Dynamics, in: Reise, K. (Ed.), *Ecological Comparisons of Sedimentary Shores*,
730 *Ecological Studies*. Springer Berlin Heidelberg, Berlin, Heidelberg, pp. 105–125.
731 https://doi.org/10.1007/978-3-642-56557-1_6

732 Pejrup, M., Mikkelsen, O.A., 2010. Factors controlling the field settling velocity of cohesive
733 sediment in estuaries. *Estuarine, Coastal and Shelf Science* 87, 177–185.
734 <https://doi.org/10.1016/j.ecss.2009.09.028>

735 Pérez, L., Salgueiro, J.L., Maceiras, R., Cancela, Á., Sánchez, Á., 2016. Study of influence of pH
736 and salinity on combined flocculation of *Chaetoceros gracilis* microalgae. *Chemical*
737 *Engineering Journal* 286, 106–113. <https://doi.org/10.1016/j.cej.2015.10.059>

738 Pottsmith, C., 2015. LISST-100X Particle Size Analyzer User’s Manual.

739 Pottsmith, C., Keir, D., 2013. LISST-100X Particle Size Analyzer User’s Manual.

740 RD Instruments, 1994. Acoustic Doppler Current Profilers User’s Manal.

741 Ren, J., Wu, J., 2014. Sediment trapping by haloclines of a river plume in the Pearl River Estuary.
742 *Continental Shelf Research* 82, 1–8. <https://doi.org/10.1016/j.csr.2014.03.016>

743 Reynolds, C.S., 2006. *Ecology of phytoplankton*. Cambridge University Press, Cambridge.

744 Shen, X., Toorman, E.A., Lee, B.J., Fettweis, M., 2018. Biophysical flocculation of suspended
745 particulate matters in Belgian coastal zones. *Journal of Hydrology* 567, 238–252.
746 <https://doi.org/10.1016/j.jhydrol.2018.10.028>

747 Sheng, G.-P., Yu, H.-Q., 2006. Characterization of extracellular polymeric substances of aerobic and
748 anaerobic sludge using three-dimensional excitation and emission matrix fluorescence
749 spectroscopy. *Water Research* 40, 1233–1239.
750 <https://doi.org/10.1016/j.watres.2006.01.023>

751 Sherwood, C.R., Aretxabaleta, A.L., Harris, C.K., Rinehimer, J.P., Verney, R., Ferré, B., 2018.
752 Cohesive and mixed sediment in the Regional Ocean Modeling System (ROMS v3.6)
753 implemented in the Coupled Ocean–Atmosphere–Wave–Sediment Transport Modeling
754 System (COAWST r1234). *Geoscientific Model Development* 11, 1849–1871.
755 <https://doi.org/10.5194/gmd-11-1849-2018>

756 Soulsby, R.L., Manning, A.J., Spearman, J., Whitehouse, R.J.S., 2013. Settling velocity and mass
757 settling flux of flocculated estuarine sediments. *Marine Geology* 339, 1–12.
758 <https://doi.org/10.1016/j.margeo.2013.04.006>

759 Spearman, J.R., Manning, A.J., Whitehouse, R.J.S., 2011. The settling dynamics of flocculating mud
760 and sand mixtures: part 2—numerical modelling. *Ocean Dynamics* 61, 351–370.
761 <https://doi.org/10.1007/s10236-011-0385-8>

762 Spencer, K.L., Manning, A.J., Droppo, I.G., Leppard, G.G., Benson, T., 2010. Dynamic interactions
763 between cohesive sediment tracers and natural mud. *Journal of Soils and Sediments* 10,
764 1401–1414. <https://doi.org/10.1007/s11368-010-0291-6>

765 Sterling, M.C., Bonner, J.S., Ernest, A.N.S., Page, C.A., Autenrieth, R.L., 2004. Characterizing
766 aquatic sediment–oil aggregates using in situ instruments. *Marine Pollution Bulletin* 48,
767 533–542. <https://doi.org/10.1016/j.marpolbul.2003.10.005>

768 Takabayashi, M., Lew, K., Johnson, A., Marchi, A., Dugdale, R., Wilkerson, F.P., 2006. The effect
769 of nutrient availability and temperature on chain length of the diatom, *Skeletonema*
770 *costatum*. *Journal of Plankton Research* 28, 831–840. <https://doi.org/10.1093/plankt/fbl018>

771 Tolhurst, T.J., Gust, G., Paterson, D.M., 2002. The influence of an extracellular polymeric substance
772 (EPS) on cohesive sediment stability, in: *Proceedings in Marine Science*. Elsevier, pp. 409–
773 425. [https://doi.org/10.1016/S1568-2692\(02\)80030-4](https://doi.org/10.1016/S1568-2692(02)80030-4)

774 Uncles, R.J., Bale, A.J., Stephens, J.A., Frickers, P.E., Harris, C., 2010. Observations of Floc Sizes
775 in a Muddy Estuary. *Estuarine, Coastal and Shelf Science* 87, 186–196.
776 <https://doi.org/10.1016/j.ecss.2009.12.018>

777 van der Lee, W.T.B., 2000. Temporal variation of floc size and settling velocity in the Dollard estuary.
778 *Continental Shelf Research* 20, 1495–1511. [https://doi.org/10.1016/S0278-4343\(00\)00034-0](https://doi.org/10.1016/S0278-4343(00)00034-0)

780 van Kessel, T., Winterwerp, H., Van Prooijen, B., Van Ledden, M., Borst, W., 2011. Modelling the
781 seasonal dynamics of SPM with a simple algorithm for the buffering of fines in a sandy
782 seabed. *Continental Shelf Research* 31, S124–S134.
783 <https://doi.org/10.1016/j.csr.2010.04.008>

784 van Leussen, W., 1988. Aggregation of particles, settling velocity of mud flocs a review, in:
785 Dronkers, J., van Leussen, W. (Eds.), *Physical Processes in Estuaries*. Springer Berlin
786 Heidelberg, Berlin, Heidelberg, pp. 347–403. https://doi.org/10.1007/978-3-642-73691-9_19

788 Verney, R., Lafite, R., Brun-Cottan, J.-C., 2009. Flocculation potential of Estuarine particles: the
789 importance of environmental factors and of the spatial and seasonal variability of
790 suspended particulate matter. *Estuaries and Coasts* 32, 678–693.
791 <https://doi.org/10.1007/s12237-009-9160-1>

792 Wan, Y., Wu, H., Roelvink, D., Gu, F., 2015. Experimental study on fall velocity of fine sediment
793 in the Yangtze Estuary, China. *Ocean Engineering* 103, 180–187.
794 <https://doi.org/10.1016/j.oceaneng.2015.04.076>

795 Wang, Ying, Jiang, H., Jin, J., Zhang, X., Lu, X., Wang, Yueqi, 2015. Spatial-Temporal Variations
796 of Chlorophyll-a in the Adjacent Sea Area of the Yangtze River Estuary Influenced by
797 Yangtze River Discharge. *International Journal of Environmental Research and Public*
798 *Health* 12, 5420–5438. <https://doi.org/10.3390/ijerph120505420>

799 Wilkinson, N., Metaxas, A., Bricchetto, E., Wickramaratne, S., Reineke, T.M., Dutcher, C.S., 2017.
800 Ionic strength dependence of aggregate size and morphology on polymer-clay flocculation.
801 *Colloids and Surfaces A: Physicochemical and Engineering Aspects* 529, 1037–1046.
802 <https://doi.org/10.1016/j.colsurfa.2017.06.085>

803 Winterwerp, J.C., 1998. A simple model for turbulence induced flocculation of cohesive sediment.
804 *Journal of Hydraulic Research* 36, 309–326. <https://doi.org/10.1080/00221689809498621>

805 Wu, B., 2015. Study of algal distribution pattern and its correlation with environmental factors in
806 Yangtze River Estuary area (in Chinese) (Ph. D. Thesis). East China Normal University,
807 Shanghai.

808 Yao, H.Y., Leonardi, N., Li, J.F., Fagherazzi, S., 2016. Sediment transport in a surface-advected

809 estuarine plume. *Continental Shelf Research* 116, 122–135.
810 <https://doi.org/10.1016/j.csr.2016.01.014>
811 Yun, C., 2004. Recent Developments of the Changjiang Estuary (in Chinese). China Ocean Press,
812 Beijing.
813 Zhao, L., Gao, L., 2019. Dynamics of dissolved and particulate organic matter in the Changjiang
814 (Yangtze River) Estuary and the adjacent East China Sea shelf. *Journal of Marine Systems*
815 198, 103188. <https://doi.org/10.1016/j.jmarsys.2019.103188>
816